CIMAC CONGRESS 25
ZURICH, MAY 19 – 23, 2025

2025 | 019

Energy,exergy, economic, and environmental (4E) analysis of S-CO2 Brayton cycle for low-speed engine

Turbochargers & Air/Exhaust Management

Liangtao Xie, Wuhan University of Technology

Jianguo Yang, Wuhan University of Technology
Xin Yang, Shanghai Marine Diesel Engine Research Institute
Xiaoling Lu, Shanghai Marine Diesel Engine Research Institute
Zheng Qin, Shanghai Marine Diesel Engine Research Institute
Xinyu Li, Shanghai Marine Diesel Engine Research Institute
Nao Hu, Wuhan University of Technology
Yu Fan, Wuhan University of Technology

ABSTRACT

As global warming, ecological degradation, and the decline of fossil fuels become more apparent, major countries and organizations are focusing on the themes of carbon peaking and carbon neutrality and have enacted relevant regulations to limit engine emissions. Obviously, making full use of the heat in the high-temperature exhaust gas can greatly enhance the efficiency of the ship's main engine and reduce the ship's operating costs. Moreover, waste heat recovery systems for ships are one of the most effective ways to reduce CO2 emissions, lower the EEDI index, and improve the economic efficiency of ocean shipping.

Five configurations of SCSBC (S-CO2 simple Brayton cycle), SCCBC (S-CO2 recuperative Brayton cycle), SCHBC (S-CO2 reheating Brayton cycle), SCIBC (S-CO2 intercooling Brayton cycle), and SCRBC (S-CO2 recompression Brayton cycle) were constructed for the exhaust gas waste heat recovery under different loads of the marine low-speed engine HHM-6EX340EF on the EBSILON platform using the bench test data. Experimental data from Sandia National Laboratories (SNL) was utilized to validate the accuracy of the model. Meanwhile, the effect of Brayton cycle parameters on exhaust gas waste heat recovery for different configurations was analyzed. The SCBC (S-CO2 Brayton cycle) was optimized from the perspectives of system configuration, cycle parameters, and working fluid preference. An indicator evaluation of the SCBC system was conducted from the perspective of 4E analysis. Parameter optimization of SCBC by MOGA and TOPSIS methods to improve the power, economy, and environment of marine diesel engines. The results showed that the combination of 100% load exhaust gas as the input, CO2-H2S as the working medium, and the recompression cycle as the system configuration is optimal. The 4E analysis showed that the optimized SCRBC has a recovered power of 178.1 kW, Brayton cycle efficiency of 19.22%, LCOE of 3.004×10-2 ($·kW-1·h-1), RCO2 of 9.68×105 (kg·a-1), and eeff of 23.29%. A technical basis was provided for realizing the application of the exhaust gas waste heat recovery S-CO2 Brayton cycle system in marine diesel engines.

1 INTRODUCTION

As global warming, ecological degradation and the decline of fossil fuels become more and more apparent, major countries and organizations are focusing on the theme of carbon peaking and carbon neutrality, and have enacted relevant regulations to limit engine emissions [1-2]. The thermal efficiency of the most advanced marine low-speed two-stroke diesel engines, which serve as the primary power source for maritime transportation, is nearly 50%. However, over half of the fuel energy is released into the environment through exhaust gas and cooling water. [3]. Making full use of the heat in the high temperature exhaust gas and cooling medium can greatly enhance the efficiency of the ship's main engine and reduce the ship's operating costs [4]. WHR system for ships is one of the effective ways to reduce CO_2 emission, lower EEDI index and improve the economic efficiency of ocean shipping. The waste heat from diesel engines presents the characteristics of multi-form, multi-grade and large span. Among them, the exhaust gas takes away the largest amount of heat, accounting for 22-30% of the heat input, and up to 300℃-500℃ [5].

The primary categories of waste heat recovery from exhaust gas include: PT (Power Turbine), ET (Electrical Turbine), WHB (Waste Heat Boiler), TEG (Thermoelectric Generator) and Waste Heat Power Cycle Technology [6-10]. PT/ET is not applicable to exhaust gas for low-speed engines due to its limitations. TEG is utilized for low-grade and small-scale heat sources. It is mostly employed in vehicles [11-12]. Existing waste heat power cycles mainly include ORC (Organic Rankine Cycle), OTC (Organic Transcritical Cycle), SRC (Steam Rankine Cycle), KC (Kalina Cycle), GC (Goswami cycle) and SCBC [13-18]. ORC, OTC, KC maximum cycle temperature is subject to the thermal stability of the working fluids, applicable to low-temperature heat sources below 200℃. SRC system composition is complex, operation and maintenance costs are high, and the power generation potential is low [19]. In exhaust gas WHR, CO_2 and exhaust gas specific heat change are similar, the heat exchange process will realize a good match. SCBC has a compact structure, strong applicability, and a wide range of power application [20].

There have been many studies so far about 4E analysis in waste heat power cycle technology. Vanaei conducted a 4E analysis of the ORC in a waste-to-energy power plant, with parametric studies of steam generator superheat temperatures, turbine inlet pressures and temperatures, to optimize the performance of the system. The exergy efficiency has been optimized to 23.77%, while the overall product cost stood at 42.94$/GJ [21]. Nandakishora combined CCUS (Carbon Dioxide Capture, Utilization and Storage) and ORC processes for energy recovery evaluation through 4E analysis [22]. Mehrabian evaluated biomass burners from four perspectives: energy, exergy, energy economy, and energy environment. The multi-objective optimization algorithms were used to further improve the objective function [23]. Wang recovered heat from the cooler of a reheat Brayton cycle through an ammonia absorption refrigeration cycle for CCHP (combined cooling, heating, and power). An evaluation model based on 4E analysis was developed and the combined cycle was optimized with multiple objectives. An average improvement of 1.11% was observed in thermal efficiency, while an average reduction of 16.21% was achieved in the total investment cost [24]. Hai used ORC to recuperated heat from the KC driven by a geothermal unit. An energy, exergy and economic analysis and optimization of the system was conducted based on a genetic algorithm using a neural network to find the optimal solution point of the LCOE (levelized cost of energy) [25]. Hu established a WP-PV-CSP (wind power-photovoltaic-concentrated solar power) system and proposed a two-tier capacity-operation synergistic optimization method to optimize the capacity and operation scheduling of the main

components of the system with the optimization objectives of LCOE and carbon dioxide emissions [26]. Khosravi used genetic algorithms to optimized turbine inlet temperature and pressure, pinch point and other parameters from the point of energy and exergy. Single and dual pressure cycles with return heaters and R123 working fluids have the highest power and lowest cost [27]. Shoaei established a power cycle for geothermal and solar energy. The process of multi-objective optimization was performed using NSGA-II (Non-dominated Sorting Genetic Algorithm) for two variables of interest: energy efficiency and capital cost. The system exhibited an energy efficiency of 50.59% and an exergy efficiency of 25.44%. The exergy loss was measured at 1537.35 kW, while the power generation amounted to 524.66 kW [28]. Shayesteh conducted an analysis of several setups of the ORC and the working fluid. This analysis focused on the recovery of energy from the main engine of a ship, specifically at the outlet of the exhaust gas, which had a temperature of 280°C. The analysis considered the impacts of 4E (exergy, energy, economic, and environmental) factors [29]. Guo performed a comprehensive analysis and comparison of S-CO_2 coal-fired power generation systems, focusing on thermodynamics and economics. The system with an intermediate cooling cycle was found to have the highest efficiency and the most cost-effective configuration [30]. Zhang utilized waste heat from the S-CO_2 cycle of a cogeneration system in a nuclear power generation system. The 4E models of S-CO_2/ORC and S-CO_2/tCO_2 (transcritical CO_2) were developed respectively. Several decision variables and five performance indicators were selected. And three trade-off solutions were discussed: economic prioritization, environmental prioritization, and economic-environmental trade-offs in search of equilibrium [31]. Xu developed a power cycle that uses tCO_2 to study the concept of generating solar thermal power at low temperatures. An assessment was conducted to determine the viability of a solar power facility that utilizes a transcritical CO_2 mixture. The evaluation focused on the energy production, efficiency, economic factors, and environmental impact (4Es). Seven organic working fluids were assessed using a two-tier decision-making framework that relied on multi-objective optimization [32]. Wang investigated two CHP (combined heat and power) cycles in which the waste heat from the S-CO_2 Brayton cycle was recovered for power generation through the tCO_2 or ORC. An economic analysis was conducted to evaluate the performance of the S-CO_2/tCO_2 cycle and compare it with the combined heat and power S-CO_2/ORC cycle [33]. Li performed a comprehensive analysis of several S-CO2 Brayton cycle configurations in a SPT (Solar Power Tower) utilizing a 4E system comparison and multi-objective optimization [34]. 4E analysis is a systematic and comprehensive evaluation method. However, the 4E analysis of the SCBC system for exhaust gas waste heat recovery in marine LSEs has not been studied so far.

An analysis was conducted to characterize the S-CO_2 Brayton cycle system for recovering waste heat from exhaust gases with bench data under different loads using an HHM-6EX340EF as the research object. The model of S-CO_2 Brayton cycle system is established, and the accuracy is verified by SNL test data. Key issues such as the exploration of the arrangement form of the Brayton cycle for exhaust gas waste heat recovery in LSEs, the optimization of CO_2-based binary working fluids and the optimization of cycle parameters have been solved, and the overall design of the Brayton cycle for exhaust gas in LSEs has been completed. Finally, the marine LSE exhaust gas S-CO_2 Brayton cycle system is evaluated from the perspectives of energy, exergy, economic and environmental. Multi-objective optimization was carried out by MOGA (Multi-objective genetic algorithm) and TOPSIS (Technique for Order Preference by Similarity to an Ideal Solution) methods to improve the power, economic and environmental friendliness of the LSE. The technical foundation is laid for realizing

the application of exhaust gas waste heat recovery S-CO_2 Brayton cycle system in marine diesel engines.

2 S-CO_2 BRAYTON CYCLE MODELING

2.1 Marine low-speed diesel engine flue gas test data

In this study, the 6EX340EF marine low-speed diesel engine is used as the research object, and its main parameters are shown in Table 1.

Table 1. Main parameters of the low-speed engine

Parameters	Values
Number of cylinders	6
Bore/mm	340
Stroke/mm	1600
Compression ratio	20.5
Fire order	1-6-2-4-3-5
Rated speed/r·min^{-1}	157
Power /kW	4896
Fuel injection	High pressure common rail (HPCR)
Main forms	Turbocharged, Intercooled, DC scavenging, Inline arrangement

The flue gas thermal properties of the low-speed engine were measured on the bench and other physical parameters were calculated as shown in Table 2. The composition of the flue gas varies from one operating condition to another and the corresponding thermal properties of the flue gas also change, which directly affects the ability to recover flue gas waste heat.

Table 2. Flue gas parameters

Load [%]	m_{ex} [kg/s]	P_{ex} [MPa]	T_{ex} [K]	H_{ex} [kJ/kg]	S_{ex} [kJ/kg·K]
25	3.14	0.04	505	228.31	4.85
50	5.90	0.13	510	233.51	4.66
75	8.58	0.24	488	210.64	4.51
100	10.60	0.32	522	245.89	4.44

Table 3 shows the measured flue gas composition of the low-speed engine. As the diesel engine load rises and the exhaust temperature rises, the composition of NO_X and CO_2 in the flue gas rises also, while the composition of HC, CO and O_2 falls, and the enthalpy of the flue gas increases significantly, while the entropy does not change much. In this study, the flue gas composition parameters measured are defined in the ship's main engine flue gas heat exchanger, and the flue gas thermal property parameters measured from the test are used as input to the S-CO_2 Brayton cycle to study the recovery potential and influencing factors of flue gas waste heat utilization in low-speed engines.

Table 3. Flue gas compositions

Load [%]	HC [ppm]	NO_X [ppm]	CO_2 [%]	CO [ppm]	O_2 [%]
25	811.7	700.7	4.0	166.6	15.1
50	672.1	727.4	4.4	70.8	14.8
75	444.7	782.3	4.6	66.1	14.8
100	333.8	812.7	5.0	48.9	14.3

2.2 Modeling and Calibration

The SCBC uses supercritical carbon dioxide, which is chemically stable and has a high thermal conductivity, as the working fluid of the cycle (31°C, 7.37 MPa). Carbon dioxide has a slight compression factor, small volume flow rate and low viscosity in the supercritical region, resulting in low compression dissipation [35]. In the S-CO_2 Brayton cycle, configuration and parameter optimization are crucial and highly correlated. Based on the simple Brayton cycle, the performance of the Brayton cycle can be changed by adding processes such as reheating, recompression, intercooling, and reheating [36]. These Brayton cycles shown in Figure 1-5 are SCSBC, SCCBC, SCRBC, SCIBC, SCRBC [37]. By comparing these S-CO_2 Brayton cycles, an arrangement suitable for LSE is found.

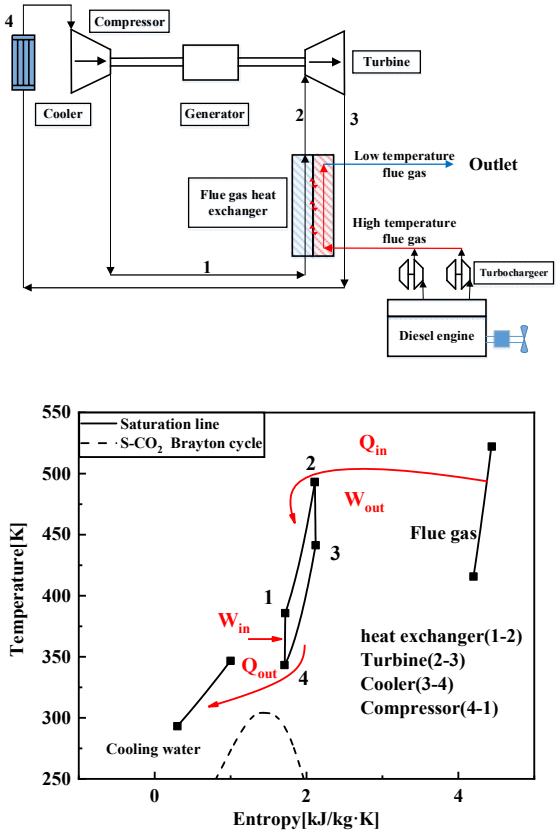

Figure 1. SCSBC system and working process

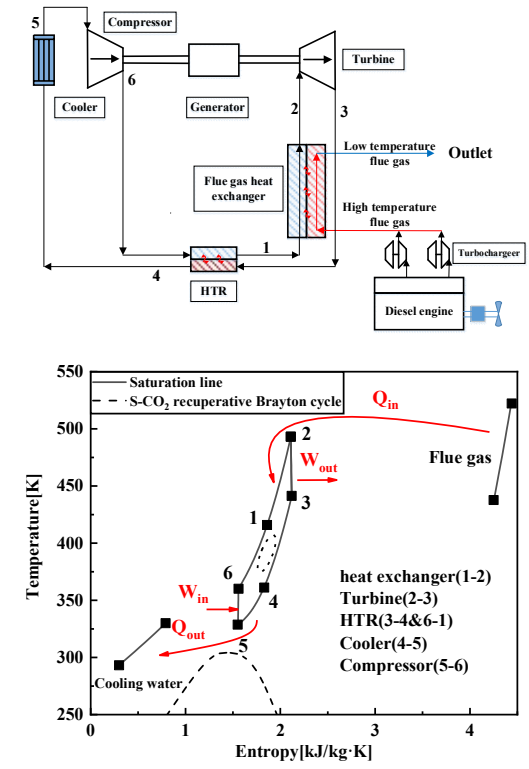

Figure 2. SCCBC system and working process

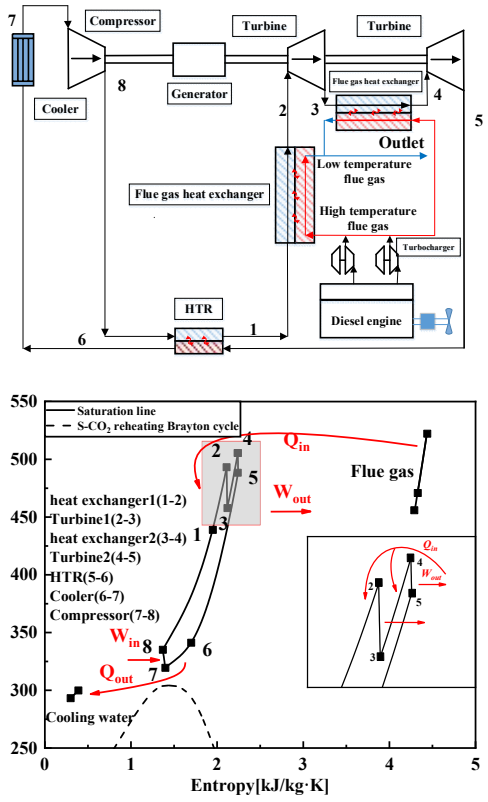

Figure 3. SCHBC system and working process

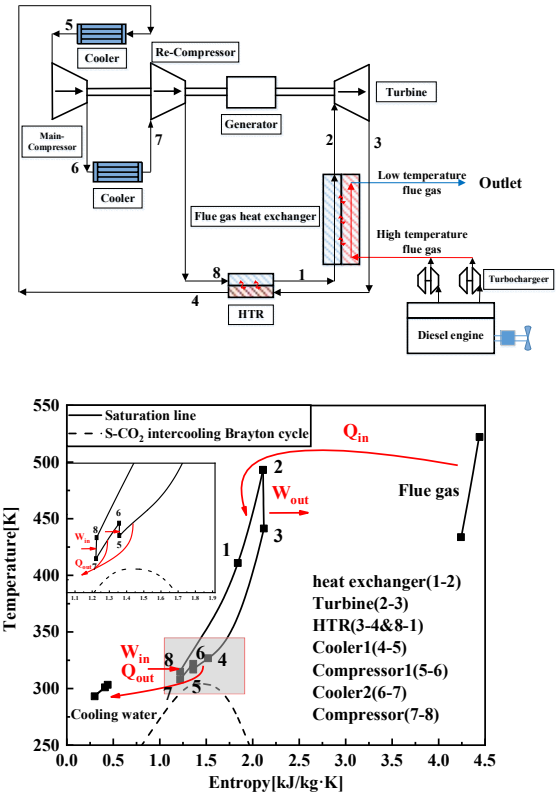

Figure 4. SCIBC system and working process

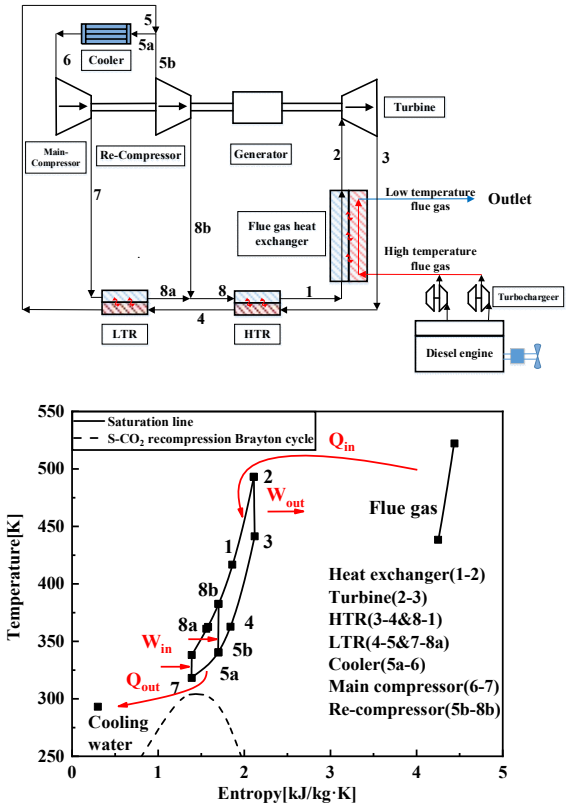

Figure 5. SCRBC system and working process

The SCBC models are developed by the Ebsilon software platform and determine the required parameters under the following assumptions.

I. The system is in a condition of equilibrium, and the changes in its kinetic and potential energy are disregarded;

II. The efficiency of the turbine and compressor isentropic efficiency;

III. Negligible heat transfer losses from the entire cycle to the environment, except for the cooler;

IV. The effectiveness of the HTR and LTR is considered;

V. The pressure drops at the cooler, and heat exchanger are not considered;

VI. The physical quantities do not vary with time;

Determining the physical characteristic of CO_2 at its threshold is challenging. The physical characteristics of CO_2 are obtained using the REFPROP 9.1 program [39], and the thermodynamic representation of each component of the cycle is shown in Table 4.

Table 4. Thermodynamic model of the components

Component	Formula
Turbine	$W_T = h_2 - h_3$
	$\eta_{T,S} = \frac{h_2 - h_3}{h_2 - h_{3,S}}$
MC	$W_{MC} = (1-r)(h_7 - h_6)$
	$\eta_{MC,S} = \frac{h_{7,S} - h_6}{h_7 - h_6}$
RC	$W_{RC} = r(h_{8b} - h_{5b})$
	$\eta_{RC,S} = \frac{h_{8b,S} - h_{5b}}{h_{8b} - h_{5b}}$
Heater	$q_{Heater} = h_2 - h_1$
HTR	$h_3 - h_4 = h_1 - \left[r h_{8b} + (1-r) h_{8a} \right]$
LTR	$h_4 - h_5 = h_{8a} - h_7$
Cooler	$q_{Cooler} = \Delta h_{Cooler} = (1-r)(h_6 - h_{5a})$
Overall	$\eta_{Total} = \frac{(1-r)(\Delta h_T - \Delta h_{MC}) + r(\Delta h_T - \Delta h_{RC})}{(1-r)(\Delta h_T - \Delta h_{MC} + \Delta h_{Cooler}) + r(\Delta h_T - \Delta h_{RC})}$

The components in the S-CO_2 recompression Brayton cycle were set up and modeled [40]. Figure 6 shows the model of the SCRBC constructed on the EBSILON platform. It includes precise values for every component as well as thermodynamic models. Workflow of S-CO_2 in blue, mechanical work in green, logic values in black, and cooling water flow in purple. The arrows on the different streams indicate the workflow of the S-CO_2 Brayton cycle. Table 5 shows the SCRBC measuring point parameters in SNL, the error between simulation and experimental values is acceptable.

Table 5. Recompression Brayton cycle measuring point parameters in SNL

Point	Mass flow (kg/s)	Pressure (MPa)	Temperature (K)
1	3318.35	19.95	782.26
2	3318.35	19.45	923.15
3	3318.35	9.28	827.07
4	3318.35	9.19	449.04
5	3318.35	9.19	361.65
5a	2391.67	9.19	361.65
5b	926.68	9.19	361.65
6	2391.67	9.09	315.15
7	2391.67	20.00	356.88
8a	2391.67	19.98	435.04
8b	926.68	19.98	436.06
8	3319.35	19.98	435.77

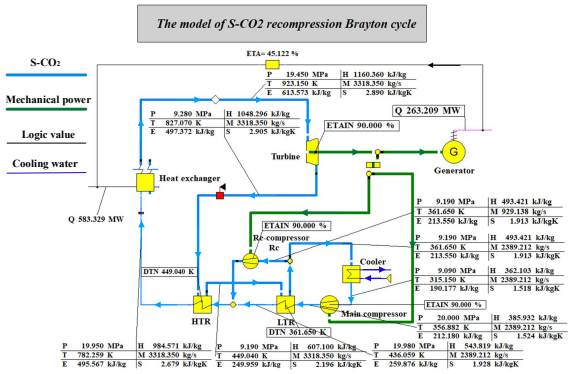

Figure 6. The Sandia model of S-CO_2 recompression Brayton cycle

Figure 7 shows the simulation value and the test value of the S-CO_2 recompression cycle equipment, the simulation value of the model and the test value of Sandia's maximum error occurs in the turbine at 4.35%, the accuracy of the model constructed to meet the requirements, and can be used for the subsequent calculation and analysis.

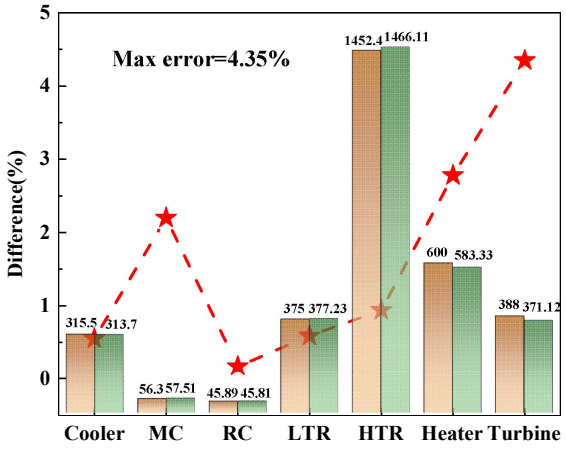

Figure 7. Comparison of simulated and experimental values of recompression equipment

3 4E MODELS OF THE BRAYTON CYCLE

4E analysis are energy, economic, exergy and environmental, and the interrelationships are shown in Figure 8. It contains the first law of thermodynamics, the second law of thermodynamics, and relevant elements of carbon trading.

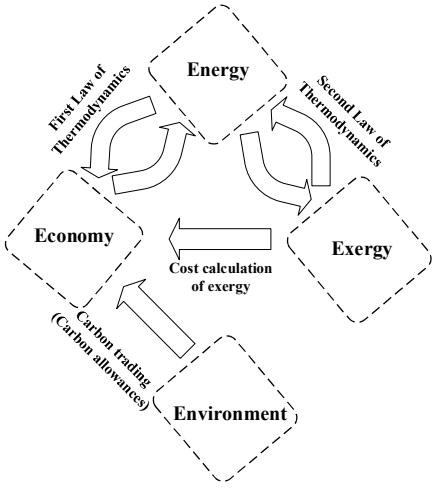

Figure 8. Interrelationships between 4E analyses

3.1 Energy model

Figure 5 displays the T-S diagram of the S-CO_2 recompression cycle at 100% load of an LSE. The saturation line of CO_2 is shown by the dotted line. The SCRBC operates as a thermodynamic system that utilizes an exhaust gas heat exchanger, Q_{in}, to

absorb heat from the exhaust gas. The system then releases heat through a cooler, Q_{out}, which cools the circulating working fluids prior to compression. The main compressor and re-compressor consume power, W_{in}, while the turbine generates power, W_{out}. The total energy loss of the circulating components is represented as Q_{loss}. The net recovered work of the system can be calculated using Equation 1.

$$W_{net} = (Q_{in} - Q_{out} - Q_{loss}) = (W_{in} - W_{out}) \quad (1)$$

The total efficiency of the system is shown in Equation 2:

$$\eta = (Q_{in} - Q_{out} - Q_{loss}) / Q_{in} \quad (2)$$

3.2 Exergy model

The SCBC exergy-loss and exergy-loss efficiencies are shown in Equation 3 and 4:

$$E_{X+} - E_{X-} = E_{X,L} \quad (3)$$

$$\eta_{exe} = \frac{E_{X-}}{E_{X+}} = 1 - \frac{E_{X,L}}{E_{X+}} \quad (4)$$

The exergy flow of SCRBC components is shown in the Figure 9, with fuel exergy in red, product exergy in blue, and output/input power in green.

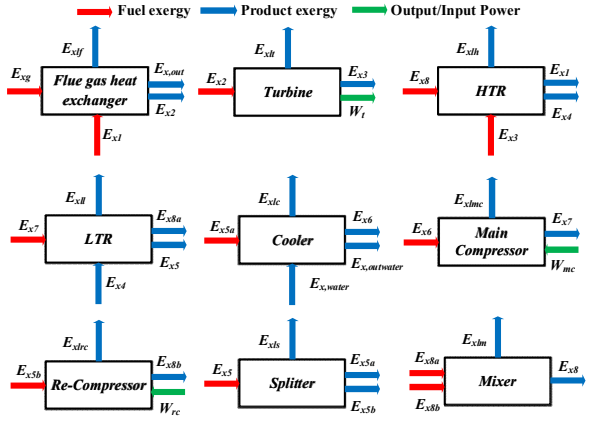

Figure 9. Exergy analysis of the SCRBC Components

3.3 Exergo-economic model

$$\sum \dot{C}_{out,i} + \dot{C}_{w,i} = \sum \dot{C}_{in,i} + \dot{C}_{q,i} + \dot{Z}_i \quad (5)$$

Where $C_{out,i}$ and $C_{in,i}$ represent the output and input exergy power cost rates associated with each flow unit, respectively, in \$/h; $C_{w,i}$ represents the output work-related heat and exergy cost rate, in \$/h; $C_{q,i}$ represents the input heat and exergy cost rate, in \$/h; and Z_i represents the cost rate associated with equipment expenditure, in \$/h.

$$\dot{C} = c\,\dot{E} \quad (6)$$

where: c is the specific exergy cost rate per flow unit, \$/KJ [50].

$$\dot{E} = \dot{E}_{ph} + \dot{E}_{ch} \quad (7)$$

The physical exergy can be expressed as follow:

$$\dot{E}_{ph} = \dot{m}[(h - h_{ref}) - T_{ref}(s - s_{ref})] \quad (8)$$

m is the mass flow rate, kg/s;

The chemical exergy can be expressed as follow:

$$\dot{E}_{ch} = \dot{m}\, e_{CO_2} \quad (9)$$

Z_i is the cost rate associated with equipment expenditure

$$\dot{Z}_i = \dot{Z}_i^{CI} + \dot{Z}_i^{OM} \quad (10)$$

$$\dot{Z}_i^{CI} = \left(\frac{CRF}{\tau}\right)\dot{Z}_i \quad (11)$$

$$\dot{Z}_i^{OM} = \left(\frac{r}{\tau}\right)\dot{Z}_i \quad (12)$$

$$CRF = \frac{i_r(1+i_r)^n}{(1+i_r)^n - 1} \quad (13)$$

Z_i^{CI} and Z_i^{OM} are associated with the annualized capital investment costs, operation and maintenance-related cost rates, in \$/h. Table 6 displays the capital investment amounts for each individual component of the system. r is a maintenance rate of 0.06, τ is annual operating hours 8200h [41].

Levelized cost of energy is the total cost per unit of energy generated over the entire life cycle of an energy project. It is a characterization indicator used to assess the cost of electricity generation over the life cycle of a system (\$/kW·h).

$$LCOP = c_{P,total} = \frac{\sum_{i=1}^{nf} c_{fi}\dot{E}_{fi} + \sum_{i=1}^{nk}\dot{Z}_k}{\sum_{i=1}^{np}\dot{E}_{pi}} \quad (14)$$

Table 6. The capital investment models for each system component

Components	Investment cost function
Cooler	$Z_h = 2143A_h^{0.514}$
MC	$Z_c = 71.1\dot{m}_{in}\frac{1}{0.92-\eta_{MC}}PR_c\ln(PR_c)$
RC	$Z_c = 71.1\dot{m}_{in}\frac{1}{0.92-\eta_{RC}}PR_c\ln(PR_c)$
LTR	$Z_h = 2681A_h^{0.59}$
HTR	$Z_h = 2681A_h^{0.59}$
Heater	$Z_h = 2143A_h^{0.514}$
Turbine	$Z_t = 479.34\dot{m}_{in}\frac{1}{0.93-\eta_t}\ln(PR_c)(1+e^{0.036T_{in}-54.4})$

3.4 Environmental model

The assessment of emissions, in terms of reducing fuel consumption rate and yearly CO_2 emissions, demonstrates the energy-saving and emission-reducing advantages of including an exhaust gas waste heat recovery system in comparison to the original engine.

LSE fuel consumption rate:

$$W_{net} = (Q_{in} - Q_{out} - Q_{loss}) = (W_{in} - W_{out}) \quad (15)$$

where m_{fuel} and W_{DE} are the hourly fuel consumption and power rating of the LSE, respectively.

LSE-SCRBC combined cycle fuel consumption rate:

$$BSFC_{DE-SRCBC} = m_{fuel} / (W_{DE} + P_{net}) \quad (116)$$

Annual CO_2 emission reductions from LSE-SCRBC combined cycle:

$$R_{CO_2-DE-SCRBC} = (P_{net} / W_{DE}) m_{fuel} \bullet \tau \bullet f_{CO_2} \quad (17)$$

f_{CO2} is the CO_2 emission factor for the complete combustion of 1kg of diesel fuel, which takes the value of 3.1863 [42].

4 THE ANALYSIS OF SCBC MODELS

4.1 4E analysis in different configuration

The waste heat recovery of the LSE under 100% load by S-CO_2 Brayton cycle in five different configurations is shown in Figure 10, among which the cycle efficiency and net recovery work of SCSBC are the lowest, and the cycle efficiency and net recovery work of SCHBC, SCIBC and SCRBC are similar and higher than those of the other two configurations. After using the S-CO_2 Brayton cycle, the efficiency of the LSE is improved, while the BSFC is decreased, in which the ability of SCHBC, SCIBC and SCRBC to improve the power of the LSE is significantly higher than that of SCSBC and SCCBC. After adopting the SCHBC as the waste heat recovery

arrangement type, the efficiency of its Brayton cycle is 20.13%, and the total power of the LSE is increased by 195.76kW, an increase in efficiency of 1.84%, and a reduction in fuel consumption rate of 7.03 (g/kW·h). After adopting SCRBC as the waste heat recovery arrangement type, its Brayton cycle efficiency is 19.22%, the total power of the LSE is increased by 178.14kW, the efficiency is increased by 1.67%, and the fuel consumption rate is reduced by 6.42 (g/kW·h).

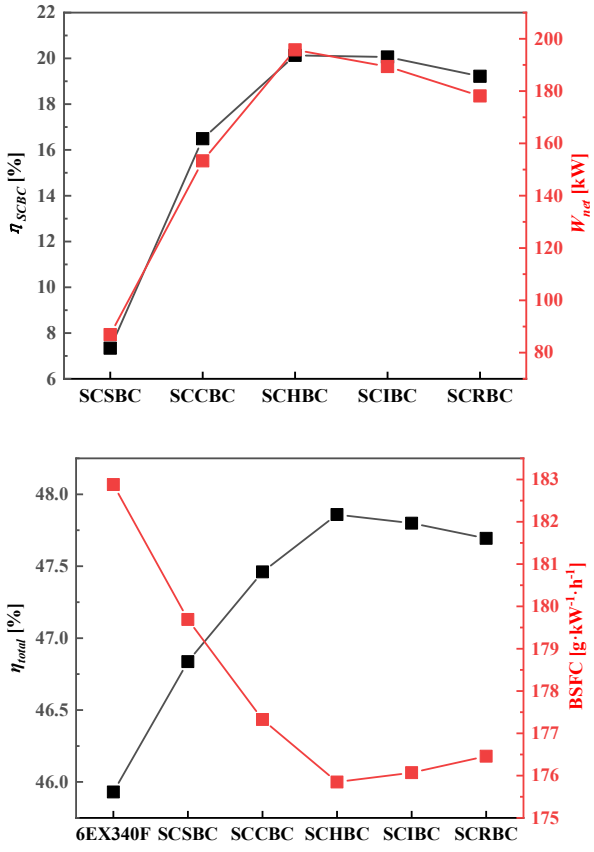

Figure. 10 Thermodynamic analysis in different configurations

The exergy loss analysis of S-CO_2 Brayton cycle of LSE under five different configurations is shown in Figure 11, in which the cooler is the component with the largest exergy loss. the SCSBC has the largest total exergy loss of 233.54 kW, with an exergy loss efficiency of 25.67%; and the SCHBC has the smallest total exergy loss of 143.02 kW, with an exergy loss efficiency of 22.85%.

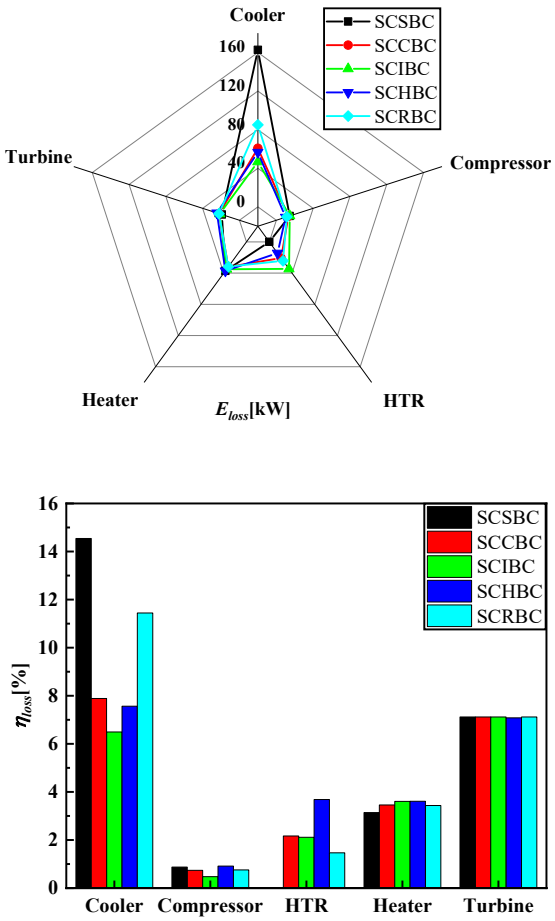

Figure. 11 Exergy analysis of the different configurations

The economic and environmental analyses of the S-CO_2 Brayton cycle at 100% load of an LSE in five different configurations are shown in Figure 12. Although the SCHBC has the best effect at 100% load, it has the highest power generation cost of 3.017 ($/kW·h) due to its complex structure and high component price. On the contrary, SCSBC has the lowest power generation cost of 2.870×10^{-2} ($/kW·h) due to its simple structure and fewer components, SCIBC has a power generation cost of 2.910×10^{-2} ($/kW·h), and SCRBC has a power generation cost of 2.892×10^{-2} ($/kW·h). From the perspective of environmental protection, the CO_2 reduction of SCHBC, SCIBC and SCRBC is obviously larger than that of SCSBC and SCCBC. Considering the power, economic and environmental protection, SCRBC is selected as the LSE configuration.

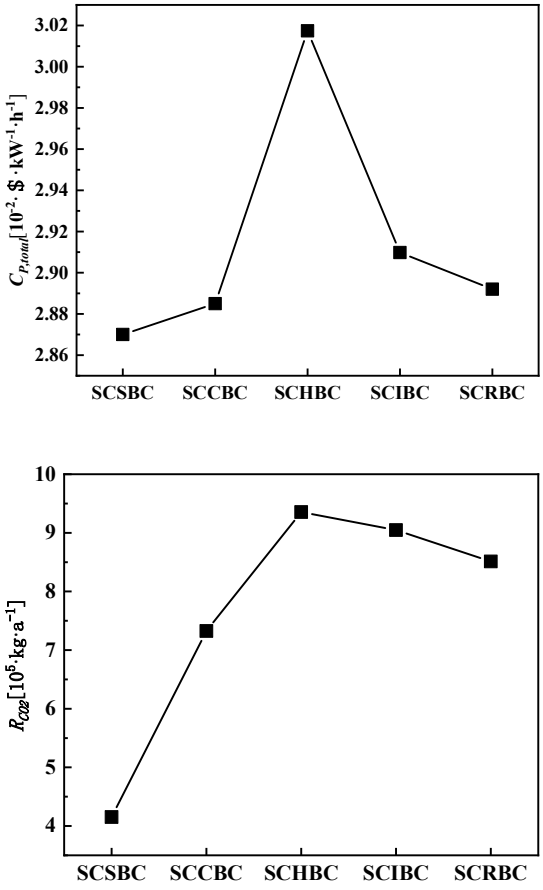

Figure. 12 Exergo-economic and environmental analysis of the different configurations

4.2 4E analysis under different loads

The SCRBC for LSE under different loads is shown in Figure 13, the capability of SCRBC for LSE under different loads is different, in which the cycle efficiency is lowest under 75% load, this is because the exhaust gas temperature under the load is the minimum of 488K, and the exhaust gas temperature determines the highest temperature of the cycle for the sensitive parameter of Brayton cycle. Therefore, the cycle efficiency is low, but due to the rising load, exhaust gas flow rate rises, the net recovery work is higher than the low and medium load. After adopting SCRBC as the waste heat recovery arrangement type, under 100% load exhaust gas, its Brayton cycle efficiency is 19.22%, the total power of LSE is increased by 178.14kW, the efficiency is increased by 1.67%, and the fuel consumption rate is reduced by 6.42 (g/kW·h). The worst effect of exhaust gas waste heat recovery was at 75% load, with a Brayton cycle efficiency of 16.55%, a total LSE power improvement of 107.16kW, a 1.33% increase in efficiency, and a 5.17 (g/kW·h) reduction in BSFC.

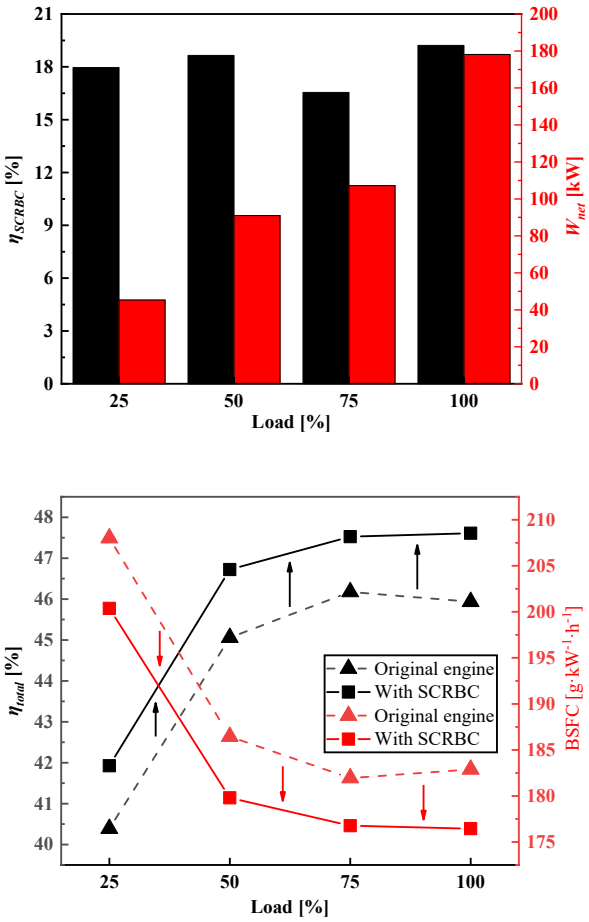

Figure. 13 Thermodynamic analysis under different loads

SCRBC analysis of LSE with four different loads of exhaust gas is shown in Figure 14, in which the cooler is still the largest exergy loss component. 100% load has the largest total exergy loss of 174.63 kW, with an exergy loss efficiency of 26.44%.

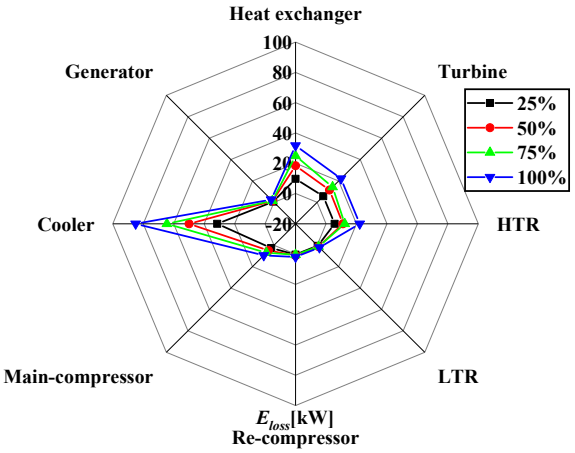

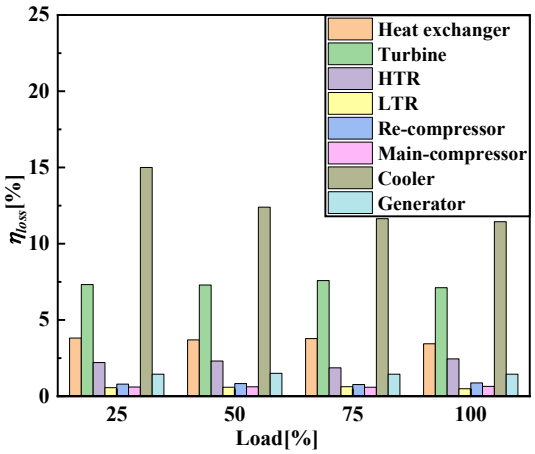

Figure. 14 Exergy analysis under different loads

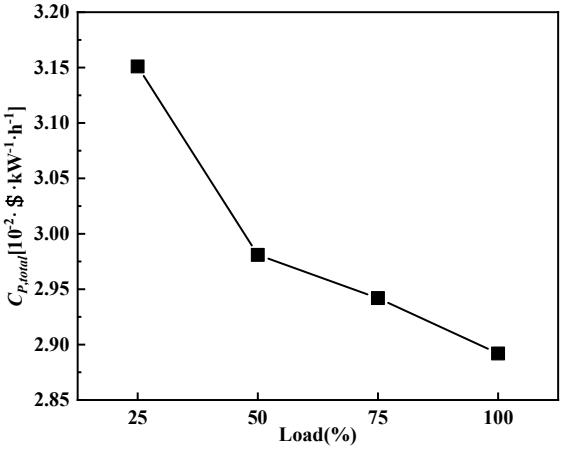

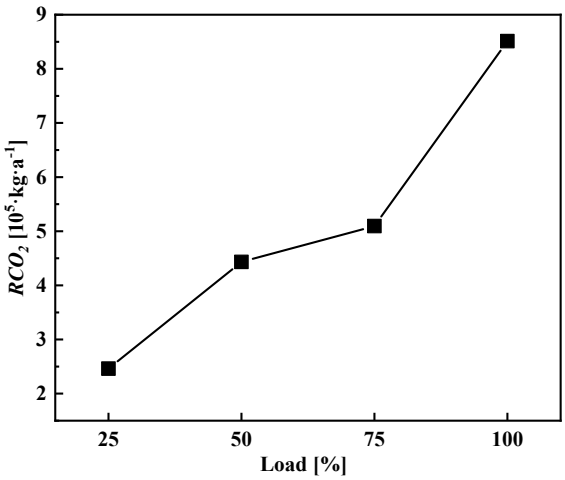

Figure. 15 Exergo-economic and environmental analysis under different loads

The economic and environmental analyses of SCRBC for the LSE under four different loads of exhaust gas are shown in Figure 15. As the load of the LSE rises, the power generation cost of the SCRBC decreases from 3.151×10^{-2} ($/kW·h) to 2.892×10^{-2} ($/kW·h), and the decrease slows down significantly at the 75% load due to the fact that at this load, the exhaust gas recovery efficiency decreases. The CO_2 reduction, on the other hand, increases from 2.46×10^5 (kg/a) to 8.51×10^5 (kg/a).

4.3 4E analysis under different working fluids

The S-CO_2 Brayton cycle for LSE at 100% load under six different working fluids is shown in Figure 16. The exhaust gas waste heat recovery ability of SCRBC is different under different working fluids, comparing with the pure CO_2 as the circulating workload, the part of exhaust gas that can be recovered decreases significantly after adding propane as the workload, and the efficiency of the Brayton cycle is improved, but the net recovery work is reduced. Although the Brayton cycle efficiency is improved, the net recovery work is reduced. In contrast, the Brayton cycle efficiency and net recovery work were further improved by adding butane, isobutane, H_2S and SO_2 to pure CO_2 as the recycling medium. The Brayton cycle efficiency is further improved by 3.09% with the

addition of H_2S to the CO_2, and the power is increased by 9.73 kW. The Brayton cycle efficiency is 22.56%, the total power of the LSE is increased by 195.76 kW, the efficiency is increased by 1.84%, and the fuel consumption rate is reduced by 7.03 (g/kW·h).

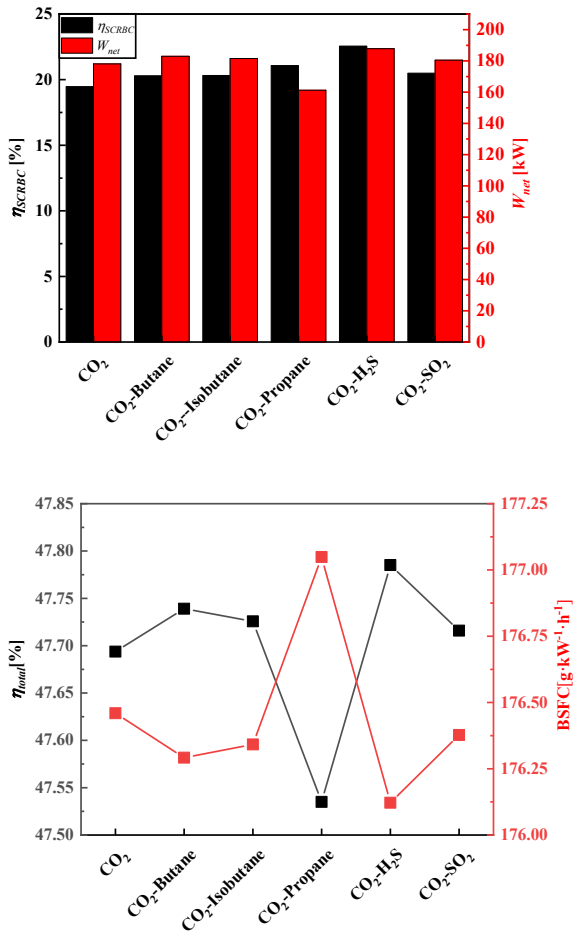

Figure. 16 Thermodynamic analysis under different working fluids

The exergy analysis of LSE at 100% load under six different working fluids is shown in Figure 17, in which the cooler is the largest exergy loss component. the total exergy loss of CO_2 is the largest, which is 162.97kW, and the exergy loss efficiency is 24.24%; the total exergy loss of CO_2-H_2S is the smallest, which is 129.90kW, and the exergy loss efficiency is 22.65%.

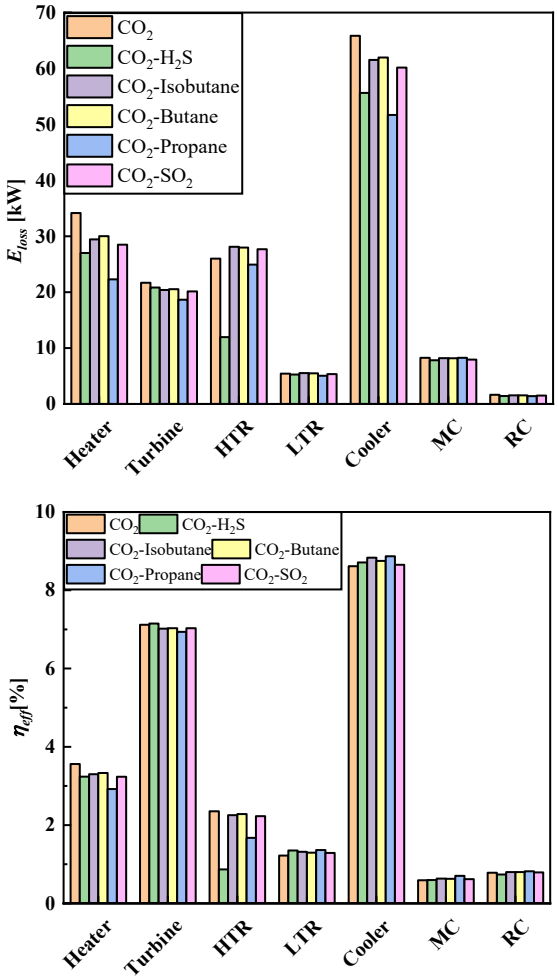

Figure. 17 Exergy analysis under different working fluids

The economic and environmental analyses of the LSE with six different working fluids are shown in Figure 18. Although the addition of different working fluids improved the exhaust gas at 100% load, the improvement was limited. The power generation cost with CO_2 as the cycle workload was 2.892 ($/kW·h). On the contrary, the power generation cost of CO_2-H_2S is 2.891×10^{-2} ($/kW·h). And from the perspective of environmental friendliness, the emission reduction of 8.98×10^5 (kg/a) for CO_2-H_2S is significantly larger than that of 7.70×10^5 (kg/a) for CO_2-Propane. Considering the power, economy and environmental protection, CO_2-H_2S was selected as the circulating working fluids for exhaust gas in the LSE.

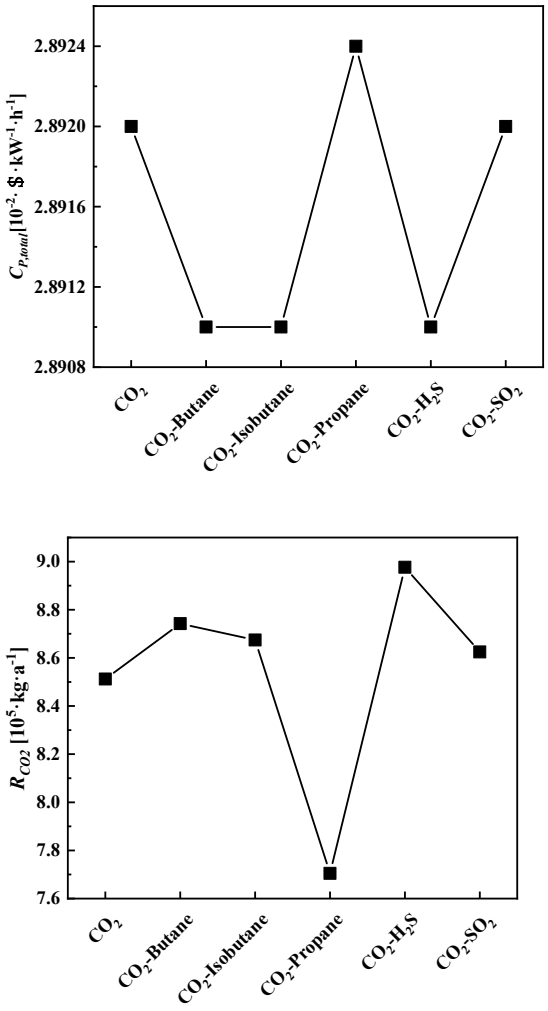

Figure. 18 Exergo-economic and environmental analysis under different working fluids

The combined distribution of the SCBC for exhaust gas in a marine LSE is shown in Table 7, where the variables are the LSE operating conditions, the cycle configuration and the working fluid. The orthogonal combination is followed by 13 cases.

Table 7. Low-speed engine exhaust gas waste heat recovery portfolio distribution

Case	Load	Configuration	Fluid
A	100%	SCSBC	CO_2
B	100%	SCCBC	CO_2
C	100%	SCHBC	CO_2
D	100%	SCIBC	CO_2
E	100%	SCRBC	CO_2
F	25%	SCRBC	CO_2
G	50%	SCRBC	CO_2
H	75%	SCRBC	CO_2
I	100%	SCRBC	CO_2-C_4H_{10}
J	100%	SCRBC	CO_2-C_4H_{10}
K	100%	SCRBC	CO_2-C_3H_6
L	100%	SCRBC	CO_2-H_2S
M	100%	SCRBC	CO_2-SO_2

Selection of optimal case of exhaust gas WHR for low-speed engine is shown in Figure 19, where Case L can be obtained as the optimal combination considering the power, exergy analysis, economy and environmental protection. For waste heat recovery of exhaust gas at 100% load of low-speed engine, this configuration of SCRBC is used, and CO_2-H_2S is used as the circulating medium. At this time, the best effect of waste heat recovery is achieved. However, the optimization of specific cycle parameters needs further analysis.

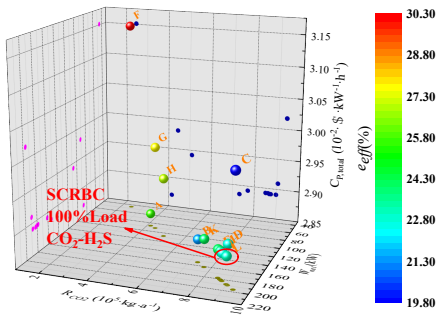

Figure. 19 Optimal case of exhaust gas WHR for low-speed engine

5 RESLUTS AND DISCUSSION

5.1 Multi-objective optimization algorithms

There are many factors affecting the performance of SCRBC, and by analyzing the effects of the cyclic parameters such as main compressor inlet pressure and temperature, cyclic maximum pressure and temperature, pressure ratio and split ratio on SCRBC, it is found that the cyclic

maximum temperature has the greatest influence, but it is limited by the temperature of the exhaust gas, and the cyclic maximum pressure is limited by the pressure resistance of the system equipment [43]. In summary, pressure ratio and split ratio were selected as the circulation variables for parameter optimization. The engine's economy and emission are improved under the premise of ensuring the engine's dynamics.

5.2 Multi-criteria decision-making methods

As shown in Figure 20, all feasible solutions including burgundy points for Pareto optimal solution black points for non-Pareto solution black are obtained with split ratio and pressure ratio as variables and cycle efficiency and net output power multi-objective maxima as objectives. By introducing ideal and non-ideal points, the optimal solution in the Pareto frontier was selected by the TOPSIS method. An evaluation metric Sdi was introduced with the Euclidean distances (Sdi^+ and Sdi^-) between the points on the Pareto as shown in Equation (18). The yellow point was the target in the range of variables when the multi-objective reached the optimization [38-39].

$$Sd_i = \frac{Sd_i^-}{Sd_i^+ + Sd_i^-} \tag{18}$$

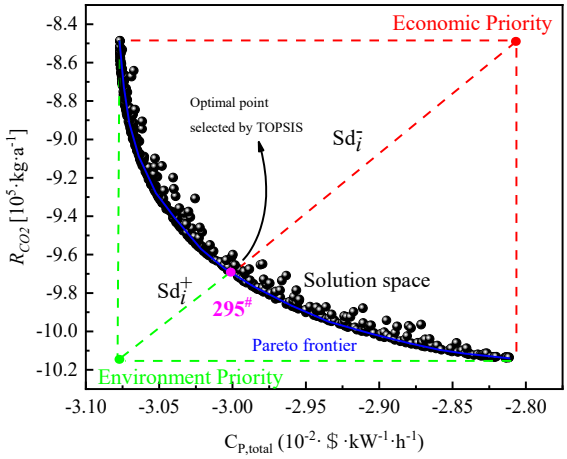

Figure. 20 Cyclic parameter optimization of Pareto front surface

As shown in Table 8, 295# case with a split ratio of 0.117 and a pressure ratio of 1.804 adopts SCRBC as the configuration and CO_2-H_2S as the working fluid for waste heat recovery of 100% load exhaust gas from the LSE, with a power generation cost of 3.004×10^{-2} ($/kW·h), an exergy loss efficiency of 23.29%, and an emission reduction of 9.68×10^5 (kg/a).

Table 8 MOGA and TOPSIS method parameters optimization for the SCRBC

ID	r	λ	$C_{p,total}$	R_{CO2}	e_{eff}
295	0.117	1.804	3.004	9.68	23.29
65	0.112	1.792	3.006	9.66	24.12
307	0.121	1.784	3.013	9.62	24.24
311	0.132	1.789	3.016	9.60	24.16
124	0.115	1.784	3.011	9.63	24.22

6. Conclusion

To recover waste heat from exhaust gases at various loads of the HHM-6EX340EF, a model of SCBC was created. Using the bench test data from the LSE, five configurations of the SCBC were produced on the EBSILON platform. The selection criteria for exhaust gas waste heat recovery in LSEs were improved by considering system architecture, cycle characteristics, and preferred operating fluids. Evaluating the SCBC system for exhaust gas in LSE from the viewpoints of energy, exergy, economic, and the environment. Optimizing the parameters of SCBC using MOGA and TOPSIS methodologies to enhance the performance, efficiency, and environmental impact of marine diesel engines.

1. The marine LSE exhaust gas S-CO_2 Brayton cycle system is evaluated from the perspectives of energy, exergy, economic and environmental. 4E analysis improves the economy and emissions of low-speed engine while ensuring their dynamics, and provides performance prediction studies for selection and design.

2. SCBC for exhaust gas waste heat recovery in

LSE has been optimized from the perspectives of system configuration, cycle parameter and working fluids optimization. With 100% load exhaust gas as input, CO_2-H_2S as the working fluids, the recycling effect was optimized under the combination of SCRBC.

3. Multi-objective optimization of the cycle was carried out by MOGA and TOPSIS methods to improve the energy, exergy, economic, and environmental of the exhaust gas waste heat recovery in LSE. 295# case with a split ratio of 0.117 and a pressure ratio of 1.804 was adopted for waste heat recovery for the LSE

4. The efficiency of the LSE has been significantly improved. The BSFC was reduced considerably by the SCBC for the exhaust gas of the LSE at 100% load. Based on the original engine, the net recovered power of exhaust gas waste heat of LSE is 178.1 kW, η_{SCRBC} is 19.22%, $C_{p,total}$ is 3.004×10^{-2} ($\cdot kW^{-1}\text{-}h^{-1}$), R_{CO2} is 9.68 ($kg\cdot a^{-1}$), and e_{eff} is 23.29%.

5. The research on the overall design of S-CO_2 Brayton cycle system for exhaust gas are carried out. The research established the technological basis for the general layout of the Brayton cycle, which is used in maritime low-speed diesel engines to recover waste heat.

6 ACKNOWLEDGMENTS

Author Contributions: Conceptualization, X.L (Xie Liangtao), Y.J(Yang Jianguo); methodology, X.L (Xie Liangtao), L.X(Li Xinyu); software, H.N (Hu Nao), Q.Z(Qin Zheng); validation, L.X(Lu Xiaoling), F.Y(Fan Yu), Y.X(Yang Xin); writing—original draft preparation, X.L (Xie Liangtao);

Acknowledgments: The authors would like to thank the editor in chief, associate editor and the anonymous referees for detailed and valuable comments that helped to improve this manuscript.

Conflicts of Interest: The authors declare no conflict of interest.

7 REFERENCES

[1] Nielsen, R.F.; Haglind, F.; Larsen, U. Design and modelling of an advanced marine machinery system including waste heat recovery and removal of Sulphur oxides[J]. Energy Conversion and Management, 2014, 85(14): 687–693.

[2] Hossain, S.N.; Bari, S. Waste heat recovery from a diesel engine using shell and tube heat exchanger[J]. Applied thermal engineering, 2013, 61(2): 355-363.

[3] Shi, L.F.; Tian, H.; Shu, G.Q. Multi-mode analysis of a CO_2-based combined refrigeration and power cycle for engine waste heat recovery[J]. Applied Energy, 2020, Vol.264: 114670.

[4] Zhang, R.Y.; Su, W.; Lin, X.X.; Zhou, N.J.; Zhao, L. Thermodynamic analysis and parametric optimization of a novel S–CO_2 power cycle for the waste heat recovery of internal combustion engines[J]. Energy, 2020, Vol.209: 11848.

[5] Hountalas, D.T.; Rogdakis, E.D.; Kouremenos, D.A.; Katsanos, C.O. Study of available exhaust gas heat recovery technologies for HD diesel engine applications[J]. International Journal of Alternative Propulsion, 2007, Vol.1: 228-249.

[6] Dolz, V.; Novella, R.; Garcia, A.; Sanchez, J. HD Diesel engine equipped with a bottoming Rankine cycle as a waste heat recovery system. Part 1: Study and analysis of the waste heat energy[J]. Applied Thermal Engineering, 2012, Vol.36(1): 269-278.

[7] Serrano, J.R.; Dolz, V.; Novella, R.; Garcia, A. HD Diesel engine equipped with a bottoming Rankine cycle as a waste heat recovery system. Part 2: Evaluation of alternative solutions[J]. Applied Thermal Engineering, 2012, Vol.36(1): 279-287.

[8] Demir, M.E.; Dincer, I. Performance

assessment of a thermoelectric generator applied to exhaust waste heat recovery[J]. Applied Thermal Engineering, 2017, Vol.120(1): 694-707.

[9] Bahrampoury, R.; Behbahaninia, A. Thermodynamic optimization and thermoeconomic analysis of four double pressure Kalina cycles driven from Kalina cycle system 11[J]. Energy Conversion and Management, 2017, Vol.152(1): 110-123.

[10] Weerasinghe, W.M.; Stobart, R.K.; Hounsham, S.M. Thermal efficiency improvement in high output diesel engines a comparison of a Rankine cycle with turbo-compounding[J]. Applied Thermal Engineering, 2010, Vol.30: 2253-2256.

[11] Yang, H.Q.; Shu, G.Q.; Tian, H.; Ma, X.N.; Chen, T.Y.; Liu, P. Optimization of thermoelectric generator (TEG) integrated with three-way catalytic converter (TWC) for harvesting engine's exhaust waste heat [J]. Applied Thermal Engineering, 2018, Vol.144: 628-638.

[12] Lan, S.; Yang, Z.J.; Chen. R.; Stobart, R. A dynamic model for thermoelectric generator applied to vehicle waste heat recovery[J]. Applied Energy, 2018, 210: 327-338.

[13] Emrullah, K.; Cuma, K.; Hüseyin, Y.; Yıldız, K.; Recep, Y.; Ali, K. Pinch point determination and Multi-Objective optimization for working parameters of an ORC by using numerical analyses optimization method[J]. Energy Conversion and Management, 2022, Vol.271: 116301.

[14] Qin, L.; Xie, G.N.; Ma, Y.; Li, S.L. Thermodynamic analysis and multi-objective optimization of a waste heat recovery system with a combined supercritical/transcritical CO_2 cycle[J]. Energy, 2023, Vol.265: 126332.

[15] Merve, A.; Hüseyin, Y.; Yıldız, K.; Ali, K.; Ali, S.; Recep, Y. Why Kalina (Ammonia-Water) cycle rather than steam Rankine cycle and pure ammonia cycle: A comparative and comprehensive case study for a cogeneration system[J]. Energy Conversion and Management, 2022, Vol.265: 115739.

[16] Feng, Y.M.; Du, Z.Q.; Shreka, M.; Zhu, Y.Q.; Zhou S.; Zhang, W.P. Thermodynamic analysis and performance optimization of the supercritical carbon dioxide Brayton cycle combined with the Kalina cycle for waste heat recovery from a marine low-speed diesel engine[J]. Energy Conversion and Management, 2020, Vol.206: 112483.

[17] Zou, Y.H.; Alghassab, M.A.; Abdulwahab, A.; Sharma, A.; Ghandour, R.; Alkhalaf, S.; Alharbi, F.S.; Abdullaeva, B.S.; Elmasry, Y. Heat recovery from oxy-supercritical carbon dioxide cycle incorporating Goswami cycle for zero emission power/heat/cooling production scheme; techno-economic study and artificial intelligence-based optimization[J]. Case Studies in Thermal Engineering, 2024, Vol.54: 104084.

[18] Zhou, T.; Liu, Z.X.; Li, X.J.; Zhao, M.; Zhao, Y.J. Thermodynamic design space data-mining and multi-objective optimization of SCO_2 Brayton cycles[J]. Energy Conversion and Management, 2021, Vol.249.

[19] Xie, L.T.; Yang, J.G. Performance Modulation of S-CO_2 Brayton Cycle for Marine Low-Speed Diesel Engine Flue Gas Waste Heat Recovery Based on MOGA[J]. Entropy, 2022, Vol.24(11): 1544.

[20] Xie, L.T.; Yang, J.G.; Hu, N.; Fan, Y.; Sun, S.C.; Dong, F.; Hu, J. Characteristics of the S-CO_2 Brayton cycle for full-scale multi-condition diesel engines[J]. Applied Thermal Engineering, 2024, Vol.236: 121484.

[21] Vanaei, P.; Jalili, B.; Hosseinzadeh, M.; Jalili, P.4E analysis of a municipal incinerator power plant with an ORC and optimization[J]. Journal of the Brazilian Society of Mechanical Sciences and Engineering, 2023, Vol.45(10).

[22] Nandakishora, Y.; Sahoo, R.K.; Murugan, S.; Gu, S. 4E analysis of the cryogenic CO_2 separation process integrated with waste heat recovery[J]. Energy, 2023, Vol.278: 127922.

[23] Mehrabian, M.J.; Manesh, M.H.K.; et al. 4E and risk assessment of a novel integrated biomass driven polygeneration system based on integrated sCO_2-ORC-AD-SOFC-SOEC-PEMFC-PEMEC[J]. Sustainable Energy Technologies and Assessments, 2023, Vol.58: 103317.

[24] Wang, Y.M.; Xie, G.N. 4E multi-objective optimization of cold electricity co-generation system based on supercritical CO_2 Brayton cycle[J]. Energy Conversion and Management, 2023, Vol.283: 116952.

[25] Hai, T.; Ali, M.A.; Chaturvedi, R.; Almojil, S.F.; Almohana, A.I.; Alali, A.F.; Almoalimi, K.T.; Alyousuf, F.Q.A.; Shamseldin, M.A. A low-temperature driven organic Rankine cycle for waste heat recovery from a geothermal driven Kalina cycle: 4E analysis and optimization based on artificial intelligence[J]. Sustainable Energy Technologies and Assessments, 2023, Vol.55: 102895.

[26] Hu, Y.D.; Zhai, R.R.; Liu, L.T.; Yin, H.; Yang, L.Z. Capacity optimization and performance analysis of wind power-photovoltaic-concentrating solar power generation system integrating different S-CO_2 Brayton cycle layouts[J]. Journal of Cleaner Production, 2023, Vol.433: 139342.

[27] Khosravi, H.; Salehi, G.R.; Azad, M.T. Design of structure and optimization of organic Rankine cycle for heat recovery from gas turbine: The use of 4E, advanced exergy and advanced exergoeconomic analysis[J]. Applied Thermal Engineering, 2019, Vol.147: 272-290.

[28] Shoaei, M.; Hajinezhad, A.; Moosavian, S.F. Design, energy, exergy, economy, and environment (4E) analysis, and multi-objective optimization of a novel integrated energy system based on solar and geothermal resources[J]. Energy, 2023, Vol.280: 128162.

[29] Shayesteh, A.A.; Koohshekan, O.; Ghasemi, A.; Nemati, M.; Mokhtari, H. Determination of the ORC-RO system optimum parameters based on 4E analysis; Water–Energy-Environment nexus[J]. Energy Conversion & Management, 2019, Vol.183: 772-790.

[30] Guo, J.Q.; Li, M.J.; Xu, J.L.; Yan, J.J.; Ma, T. Energy, exergy and economic (3E) evaluation and conceptual design of the 1000 MW coal-fired power plants integrated with S-CO_2 Brayton cycles[J]. Energy Conversion and Management, 2020, Vol.211: 112713.

[31] Zhang, D.; Zhang, H.C.; Luo, Y.; Zhao, S.T.; Miao, X.Y. Exploring energetic, exergetic, economic and environmental (4E) performance of waste heat power generation in nuclear power plant systems: A perspective of pattern recognition[J]. Journal of Cleaner Production, 2023, Vol.425: 138911.

[32] Xu. X.; Wu, C.; Liu, C.; Xu, X.X. Feasibility assessment of trough concentrated solar power plants with transcritical power cycles based on carbon dioxide mixtures: A 4E analysis and systematic comparison[J]. Journal of Cleaner Production, 2024, Vol.436: 140603.

[33] Wang, X.R.; Dai, Y.P. Exergoeconomic analysis of utilizing the transcritical CO_2 cycle and the ORC for a recompression supercritical CO_2 cycle waste heat recovery: A comparative study[J]. APPLIED ENERGY, 2016, Vol.170: 193-207.

[34] Wang, K.; Li, M.J.; Guo, J.Q.; Li, P.W.; Liu, Z.B. A systematic comparison of different S-CO_2 Brayton cycle layouts based on multi-objective optimization for applications in solar power tower plants[J]. APPLIED ENERGY, 2018, Vol.212: 109-121.

[35] Son, S.M.; Heo, J.Y.; Lee, J.I. Prediction of inner pinch for supercritical CO_2 heat exchanger using Artificial Neural Network and evaluation of its impact on cycle design[J]. Energy Conversion and Management, 2018, Vol.163(1): 66-73.

[36] Kumar, B.R.; Saravanan, S.; Rana, D.; Nagendran, A. Combined effect of injection timing and exhaust gas recirculation (EGR) on performance and emissions of a DI diesel engine fueled with next-generation advanced biofuel-Diesel blends using response surface methodology. Energy Conversion and Management. 2016, 123, 470-486.

[37] Jing, R.; Zhu. X.Y.; Zhu, Z.Y.; et al. A multi-objective optimization and multi-criteria evaluation integrated framework for distributed energy system optimal planning[J]. Energy Conversion and Management, 2018, Vol.166(1):445-462.

[38] Wang, D.; Xie, X.; Wang, C.; et al. Thermo-economic analysis on an improved coal-fired power system integrated with S-CO_2 brayton cycle[J]. Energy, 2021, 220: 119654.

[39] Merchán, R. P.; Sánchez Santos, M. J.; García-Ferrero, J.; et al. Thermo-economic and sensitivity analysis of a central tower hybrid Brayton solar power plant[J]. Applied Thermal Engineering, 2021, 186: 116454.

[40] Wright, S.A.; Radel, R.F.; Vernon, M.E.; et al. Operation and analysis of a supercritical CO_2 Brayton cycle[R]. Sandia National Laboratories SAND2010-0171, 2010.

[41] Sleiti, A.K.; Al-Ammari, W.A. Energy and exergy analyses of novel supercritical CO_2 Brayton cycles driven by direct oxy-fuel combustor[J]. Fuel, 2021, Vol.294: 120557.

[42] Yao, L.C; Zou, Z.P. A one-dimensional design methodology for supercritical carbon dioxide Brayton cycles: Integration of cycle conceptual design and components preliminary design[J]. Applied Energy, 2020, Vol.276: 115354.

[43] Wolf, V.; Bertrand, A.; Leyer, S. Analysis of the thermodynamic performance of transcritical CO_2 power cycle configurations for low grade waste heat recovery[J]. Energy Reports, 2022, Vol.8: 4196-4208.